

# Comparison of Three Turbulence Models in Wear Prediction of Multi-Size Particulate Flow through Rotating Channel

Pankaj K. Gupta and Krishnan V. Pagalthivarthi

**Abstract**—The present work compares the performance of three turbulence modeling approach (based on the two-equation  $k-\varepsilon$  model) in predicting erosive wear in multi-size dense slurry flow through rotating channel. All three turbulence models include rotation modification to the production term in the turbulent kinetic-energy equation. The two-phase flow field obtained numerically using Galerkin finite element methodology relates the local flow velocity and concentration to the wear rate *via* a suitable wear model. The wear models for both sliding wear and impact wear mechanisms account for the particle size dependence. Results of predicted wear rates using the three turbulence models are compared for a large number of cases spanning such operating parameters as rotation rate, solids concentration, flow rate, particle size distribution and so forth. The root-mean-square error between FE-generated data and the correlation between maximum wear rate and the operating parameters is found less than 2.5% for all the three models.

**Keywords**—Rotating channel, maximum wear rate, multi-size particulate flow,  $k-\varepsilon$  turbulence models.

## I. INTRODUCTION

**P**REDICTION of particulate flow-induced erosion in centrifugal slurry pumps is of tremendous economic significance to the slurry transportation industry. The wet-end components of a centrifugal slurry pump such as the impeller, casing and side-liners are usually made up of hard cast iron alloys that are hard to repair by welding. For optimal use, one of the consideration is to obtain nearly uniform wear rate over the wetted surface so that there are no undesirable premature local failures due to erosion. In addition to the cost of replacing a worn out component, downtime in production is a serious consideration in many applications [1]. It has been reported [2] that an unscheduled downtime can cost in excess of 100,000 US\$ per hour for a SAG mill slurry pump operating under the most severe of wear conditions. Of all the wet-end components of a centrifugal slurry pump, erosion wear of the impeller has greater influence on the pump performance [3]. The peripheral speed of an impeller that relates directly to the head produced is a key parameter

affecting wear. Generally, wear rate increases with increase in required rotary speed [3].

Erosion wear prediction is generally carried out in three steps [1]: (i) computation of two-phase flow field within the component, (ii) correlation of the local flow conditions (velocity and concentration) near the wear surface to the local wear rate *via* a suitable wear model, and (iii) empirical determination of the wear coefficient. Thus, computation of two-phase flow field forms the vital step.

Computation of flow field through rotating passages (such as impellers) is a difficult task due to the complex nature of flow resulting from system rotation, three dimensional geometry, presence of secondary flow, turbulence modification and so forth. In addition, the presence of particles further complicates matters. The mean flow field and turbulence can both be greatly affected by the particles. Moreover, many industrial slurries are dense with a wide particulate size distribution which cannot be accurately represented by a single particle diameter; multiple size classes must be used [4]-[6].

Using simplified analysis of considering the case of multi-size dense slurry flow in a two-dimensional straight rotating channel, several studies [7]-[11] have addressed some of the various features of the dense particulate flow *viz.*: (1) the broad particle size distribution; (2) mathematical modeling of two-dimensional multi-size particulate flow in rotating frame of reference using the continuum mechanical model, taking into account (3) the most important interactive forces (like drag, lift, virtual mass etc.) between the multiple species (phases); (4) numerical methodology employs Galerkin finite element technique using  $Q_1Q_0$  elements; and finally (5) turbulence modeling using Coriolis- and concentration-modified  $k-\varepsilon$  model.

Concentration-modified eddy viscosity [12]-[13] models have been in use in turbulent slurry flow modeling. In such models, first the carrier-phase flow field (in the absence of particles) and its eddy viscosity are computed. The presence of the particulate phase alters the eddy viscosity of the carrier-phase due to particle-fluid interactions. In addition, the particle-particle interactions also affects the eddy viscosity (or diffusivity) of the solid particles. Both these interactions are incorporated (e.g., [13]-[14]) in the concentration-modified eddy viscosity model.

P. K. Gupta is with Raghu Engineering College, Visakhapatnam, India – 531162 (corresponding author phone: +91-8922-248001; fax: +91-8922-248011; e-mail: pankajkgupta@gmail.com).

K. V. Pagalthivarthi is with GIW Industries Inc., Grovetown, GA – 30813, USA.

Thus, mixing-length based concentration-modified eddy viscosity models have been successfully employed to compute quasi three-dimensional two-phase flow in pump casings [15], concentration distribution in impellers [16]-[17], free surface flow in rotating channels [18], and recently in multi-size particulate flow in stationary channel [6] and pipelines [5]. Though mixing-length models with modification for rotation have been used [19]-[20] in single phase flow, they lack the greater generality of  $k-\varepsilon$  models. In turn, rotation modification to the standard (industry-popular)  $k-\varepsilon$  model has been shown [21] to reasonably predict mean flow of simple fluids through rotating channels.

The Coriolis- and concentration-modified  $k-\varepsilon$  model has been successfully employed to compute two-phase flow field in straight rotating channel [7], [8], [22]. In a recent finite element-based study [23], some of the other variants of the industry popular two-equation  $k-\varepsilon$  based turbulence models are explored. The study discusses in detail the implementation and validation of these variants (of the two-equation  $k-\varepsilon$  turbulence models) in computing multi-size particulate flow field in a rotating channel.

Thus, the objective of the present study is to implement and compare other variants [23] of the industry-popular  $k-\varepsilon$  model in erosion wear prediction of multi-size particulate flow in rotating channel. The present study uses three different turbulence modeling approach based on the two-equation  $k-\varepsilon$  model. All the three turbulence modeling approach incorporates a rotation modification to the production term in the turbulent kinetic energy [23].

In the first modeling approach [7], the eddy viscosity field of the pure carrier phase is obtained using the rotation-modified two-equation  $k-\varepsilon$  model. The eddy viscosity thus obtained is modified for concentration. This approach (hereafter referred to as Pure Carrier-phase based Eddy Viscosity Model or PCEVM) has been used to simultaneously retain the generality of the  $k-\varepsilon$  model and the simplicity of the concentration-modified eddy viscosity models. In the other two models, a variant of the standard  $k-\varepsilon$  model adopted for the mixture [24] is used. The two modeling approaches basically rely on the mixture-based turbulence model [25], and are hereafter referred to as Mixture-based Eddy Viscosity Models (MEVM-I and MEVM-II, respectively) in the present study. Unlike the rotation-modified  $k-\varepsilon$  model for the pure-carrier phase (PCEVM), the mixture-based eddy viscosity models (MEVM-I and MEVM-II) directly computes the eddy viscosity of the mixture, *i.e.*, the equations governing the mixture flow field are closed by obtaining the mixture eddy viscosity computed from the rotation-modified  $k-\varepsilon$  model for the mixture. Once the mixture eddy viscosity is obtained, the eddy viscosities (and diffusivities) of all constituent phases are calculated. The effect of concentration is integrally introduced in these (MEVM-I and MEVM -II) models. The essential difference between MEVM-I and MEVM-II lies in the approach in

obtaining the turbulent eddy viscosities of the individual phases (carrier-phase and solid species) from the eddy viscosity of the mixture.

In a recent work [22], erosion wear prediction in dense multi-size particulate flow through rotating channel has been numerically investigated using the Coriolis- and concentration-modified (PCEVM) model for turbulence. The wear models used in this study account for the broad particle size distribution. It is reported that the relationship that exists between the different operating parameters on the local flow conditions (and hence wears rates) is quite complex. The maximum wear rate usually occurs either at the inlet or at the exit subject to the operating parameters.

In the present study therefore, the performance of other variants of the two-equation  $k-\varepsilon$  turbulence models (mixture-based eddy viscosity models) are compared against the PCEVM in erosion wear prediction of multi-size particulate flow through rotating channel. The two distinct features of the present study that distinguishes it from the previous studies [22], [23] are as follows:

- (a) The comparison of predicted results of erosion wear using the three turbulence modeling approach are presented for a large number of cases (432 parametric runs) over such operating parameters as flow rate, particle size distribution, average overall concentration and rotational speeds; and
- (b) Based on the dataset obtained from the 432 cases (parametric runs), correlations are developed for the maximum wear rates for each model. These correlations are developed using the finite element (FE) generated data using each of the three turbulence models.

As in the previous studies [7], [8], [22], [23], the mathematical modeling is based on the continuum-mechanical model whereas the numerical modeling employs Galerkin finite element methodology with  $Q_1Q_0$  elements. For a detailed discussion on mathematical and numerical formulation, please refer [7]. The study [7] uses PCEVM turbulence approach in erosion wear prediction. Thus, in the present study, erosion wear prediction using PCEVM approach is compared with two other turbulence approach MEVM-I and MEVM-II. For the details pertaining to the implementation of mixture-based turbulence modeling approach, please refer [23].

## II. IMPACT WEAR RATE

Impact wear rate is correlated to the kinetic energy flux of the particles as

$$\dot{W}_I = \frac{\rho_s C_s V_s^3}{E_I(\alpha)}, \quad (1)$$

where  $\rho_s$  is the solids density,  $C_s$  is particle concentration,  $V_s$  is particle impact velocity and  $E_I(\alpha)$  is the impact wear coefficient as a function of the impact angle  $\alpha$ . Note that  $\rho_s C_s V_s$  is the mass flux and  $V_s^2$  is the kinetic energy per unit

mass of the particles.

For multi-size particle flow, the overall impact wear rate is likely to be influenced by all the representative particle sizes. Thus the total impact wear rate is given as [22]

$$\dot{W}_I = \sum_{k=1}^N \frac{\rho_k C_k V_k^3}{E_{Ik}(\alpha_k)}, \quad (2)$$

where  $\rho_k$ ,  $C_k$  and  $V_k$  are the density, concentration and velocity of particle size class  $k$ , and  $E_{Ik}(\alpha_k)$  is the specific energy coefficient for impact wear for the  $k^{\text{th}}$  species. The velocity  $V_k$  is given by

$$V_k = \sqrt{u_k^2 + v_k^2}, \quad (3)$$

where  $u_k$  and  $v_k$  are  $x$ - and  $y$ - components of particle velocity,  $V_k$ , and the angle of impact,  $\alpha_k = \tan^{-1}(|v_k|/|u_k|)$ .

Based on experiments [26], the particle size dependence of  $E_I$  ( $J/m^3$ ) may be written as

$$E_I(\alpha_k, d_{pk}) = C_{adj} E_I(\alpha_k), \quad (4)$$

where  $d_{pk}$  is the particle diameter of the  $k^{\text{th}}$  species;  $E_I(\alpha_k)$  is the value for  $d_{pk} = 160 \mu\text{m}$  particles, and  $C_{adj}$  is an adjustable factor given as

$$C_{adj} = A_{im} [1.65 d_{pk} + C_{im}]^{n_{im}} + B_{im}, \quad (5)$$

with  $A_{im}$ ,  $B_{im}$ ,  $C_{im}$  and  $n_{im}$  being determined experimentally. For a specific Ni-Cr white iron alloy material and sand slurries, the recommended values are [26]

$$\begin{aligned} A_{im} &= 8.578 \times 10^{10}, \\ B_{im} &= 3.645 \times 10^{-2}, \\ C_{im} &= 490, \text{ and} \\ n_{im} &= -3.668. \end{aligned} \quad (6)$$

In (5),  $d_{pk}$  is in micrometers. Thus for the multi-size particulate slurry the total impact wear rate [22]

$$\dot{W}_I = \sum_{k=1}^N \frac{\rho_k C_k V_k^3}{E_I(\alpha_k, d_{pk})}. \quad (7)$$

Note that the calculations presented in this study are restricted to the specific material whose wear coefficient is defined by (4-6).

In a rotating channel the particle velocities are generally directed towards the pressure side of the channel. Thus, directional impact is likely to occur mainly on the pressure side wall of the channel. In the present study, therefore, directional impact wear on the channel suction side is assumed to be negligible. Fig. 1 shows the schematic of the rotating channel, where  $H$  is the height and  $L$  is the physical length of the channel.

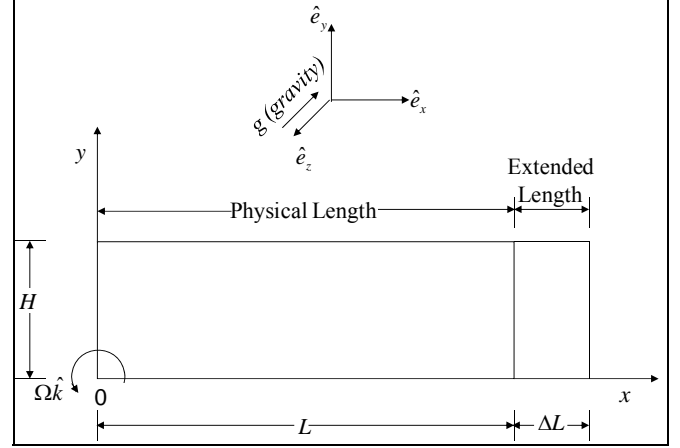


Fig.1. Computational domain of the physical problem

### III. SLIDING WEAR RATE

Sliding wear is related to the abrading action of solids against the wearing surface. The frictional power associated with the particles in such a sliding action is used to relate the sliding wear rate *via* the specific energy of sliding.

For multi-size particulate flow, the sliding wear rate is computed as the summation of sliding wear rates due to each size class. Thus, the sliding wear rate for multi-size particulate flow is expressed as

$$\dot{W}_{SL} = \sum_{k=1}^N \frac{C_k \tau_k u_k}{E_{SP}(d_{pk})}, \quad (8)$$

where  $\tau_k$ ,  $C_k$  and  $u_k$  are, respectively, the shear stress, concentration and the tangential velocity of particulate species ' $k$ '. The particle size-dependent specific energy for sliding,  $E_{SP}(d_{pk})$  [27, 28] is given as

$$E_{SP}(d_{pk}) = 10^8 \left[ A_{sl} \{d_{pk} + C_{sl}\}^{n_{sl}} + B_{sl} \right], \quad (9)$$

where,  $A_{sl}$ ,  $B_{sl}$ ,  $C_{sl}$  and  $n_{sl}$  are empirically determined constants for a particular material (and  $d_{pk}$  is in microns). In the present study, these empirical constants are chosen (for a specific white iron alloy material) as

$$\begin{aligned} A_{sl} &= 4.236 \times 10^{14}, \\ B_{sl} &= 180, \\ C_{sl} &= 490, \text{ and} \\ n_{sl} &= -3.861. \end{aligned} \quad (10)$$

The wall shear stress  $\tau_k$ , is computed as

$$\tau_k = \rho_k u_{\tau k}^2, \quad (11)$$

where  $u_{\tau k}$  is the friction velocity which is computed using the wall functions and the known (already computed) velocity field.

The total wear rate is given as the sum of  $\dot{W}_I$  and  $\dot{W}_{SL}$ .

### IV. DISCUSSION OF RESULTS

Erosion wear is a complex boundary phenomenon and is

greatly affected due to the local flow conditions in the vicinity of the wall, particularly the solids velocity and concentration distributions adjacent to the channel walls. A comprehensive discussion on wear models, validation and the effects of various operating parameters on the erosion wear in rotating channel is presented in [22].

As aforementioned, in the present study, predicted results of erosion wear using the three turbulence modeling approach are presented for a large number of cases (432 parametric runs). The database obtained from the FE-predicted results is used further to develop correlations for maximum wear rates.

Six particle size distributions (PSDs), three average (overall) inlet concentrations, four average inlet velocities (or Reynolds number) and six rotational speeds (or rotation number) are considered. Thus a total of

$6(\text{PSD}) \times 3(C_{avg}) \times 4(\text{Re}_H) \times 6(\text{Ro}_H)$  (= 432) cases are run using PCEVM, MEVM-I and MEVM-II codes separately. Table I shows the range of values of the operating parameters.

PSDs	$C_{avg}$	$\text{Re}_H$	$\text{Ro}_H$
Slurry A1	8 %	$1.75 \times 10^5$	0.02
Slurry A2			0.04
Slurry B1	12 %	$2.5 \times 10^5$	0.06
Slurry B2			0.08
Slurry C1	18 %	$5 \times 10^5$	0.10
Slurry C2			0.12

TABLE II REPRESENTATIVE PARTICLE DIAMETERS OF SIX SIZE CLASSES OF SLURRIES A, B AND C

	Size Class 1 ( $\mu\text{m}$ )	Size Class 2 ( $\mu\text{m}$ )	Size Class 3 ( $\mu\text{m}$ )	Size Class 4 ( $\mu\text{m}$ )	Size Class 5 ( $\mu\text{m}$ )	Size Class 6 ( $\mu\text{m}$ )
Slurry-A	50	100	150	250	500	750
Slurry-B	40	125	200	400	700	900
Slurry-C	38	91	128	180	255	738

TABLE III PERCENTAGE WISE CONCENTRATION DISTRIBUTION OF THE SIX SIZE CLASSES

	Slurry-A		Slurry-B		Slurry-C	
	C1	C2	C1	C2	C1	C2
$d_w$ (in $\mu\text{m}$ )	187.5	342.5	320	394.5	160.6	180.5
Size Class 1	30	10	25	16.67	5	10
Size Class 2	25	15	20	16.67	15	10
Size Class 3	15	15	15	16.67	40	30
Size Class 4	15	20	15	16.67	25	30
Size Class 5	10	20	15	16.67	10	15
Size Class 6	5	20	10	16.67	5	5

Three (PSDs) different slurries (A, B, C) with the representative particle diameters of the six size classes are used in the study as shown in Table II. For each slurry, two different sets of individual concentrations of the six species are considered. Thus there are six distinct PSDs or slurries under consideration.

The concentrations (as a percentage of the overall concentration) of each size class for the three slurries are shown in Table III. For convenience, the weighted mean diameter of each of the six PSDs is also shown in Table III. Slurry A-C1 with concentration distribution (weighted mean diameter,  $d_w = 187.5 \mu\text{m}$ ) is small-particle dominated since the two smallest size classes account for 55% of the overall concentration. Similarly, Slurry A-C2 ( $d_w = 342.5 \mu\text{m}$ ) is large-particle dominated since the three largest size classes account for 60% of the overall concentration. Slurry B-C2 has a uniform share of all six classes. Slurry C-C1 and C-C2 are

both dominated by intermediate-size particles. In subsequent discussions, the slurries are referred to simply as A1, A2, B1, B2, C1 and C2 instead of as A-C1, A-C2 etc.

In all the cases, the density of all six size classes is  $2680 \text{ kg/m}^3$ . In general, both sliding and impact wear rates are computed using the particle size-dependent specific energy coefficients in the wear models (refer (7) and (8), respectively). The wear coefficients used are for the combination of sand particles and white iron alloy wear material.

#### A. Comparison of Turbulence Models for Maximum Wear Rates and Mass Loss

This section presents a comparison of the overall results (of 432 parametric runs) using all three models. Two criteria are used for this comparison, viz., (i) the maximum predicted wear rate and (ii) the rate of mass loss (in mg/hr) along the channel pressure side using the three turbulence models for

all 432 cases. The total maximum wear rate is computed as

$$\dot{W}_{\max} = (\dot{W}_{SL} + \dot{W}_I)_{\max} \quad (12)$$

As discussed previously, at the suction side of the channel the wear is only due to sliding. The maximum (total) wear rate in (12) is computed only at the pressure side of the channel, since wear rates are always higher on the pressure side [22]. The mass loss ( $\Delta\dot{m}$ ) along the pressure side channel wall is related to wear rate as

$$\Delta\dot{m} = \int_{x=0}^{x=L} \rho_{wm} (\dot{W}_{SL} + \dot{W}_I) b dx, \quad (13)$$

where  $\rho_{wm}$  is the density of the wear material (taken as  $7700 \text{ kg/m}^3$  for white-iron alloy material), and  $b$  and  $L$  are channel width and length, respectively. The width is assumed to be unity.

A comparison of maximum (total) wear rate (in microns/hr) and mass loss (in mg/hr) along the channel pressure side computed using PCEVM and MEVM-I is presented in Fig. 2. The line of 100% accuracy ( $y=x$ ) and the best fit line ( $y=1.0252x$ ) are also plotted. The regression coefficients ( $r^2$ ) for the two lines are  $r^2 = 0.9539$  and  $r^2 = 0.9548$ , respectively, indicating very good agreement between the two predictions for maximum wear rates. The results of computed rate of mass loss also show reasonable agreement between the predictions using PCEVM and MEVM-I.

In Figs. 3 and 4, similar comparisons are made for PCEVM vs. MEVM-II and MEVM-I vs. MEVM-II, respectively. The predictions using PCEVM and MEVM-II are seen to be in very good agreement. It may be concluded that the agreement between PCEVM and MEVM-I is best for maximum wear rate. This reinforces the conclusion of the comparison of concentration and mixture velocity using PCEVM and MEVM-I presented in [23].

The deviation in the results of mass loss particularly at higher wear rates is possibly due to the cumulative effect of averaging wear rates over the entire length of the channel whereas the maximum wear rate occurs at a unique point. It is also shown that the disagreement between the results of the two models occur for large wear rates, *i.e.* larger rotation rates and flow rates.

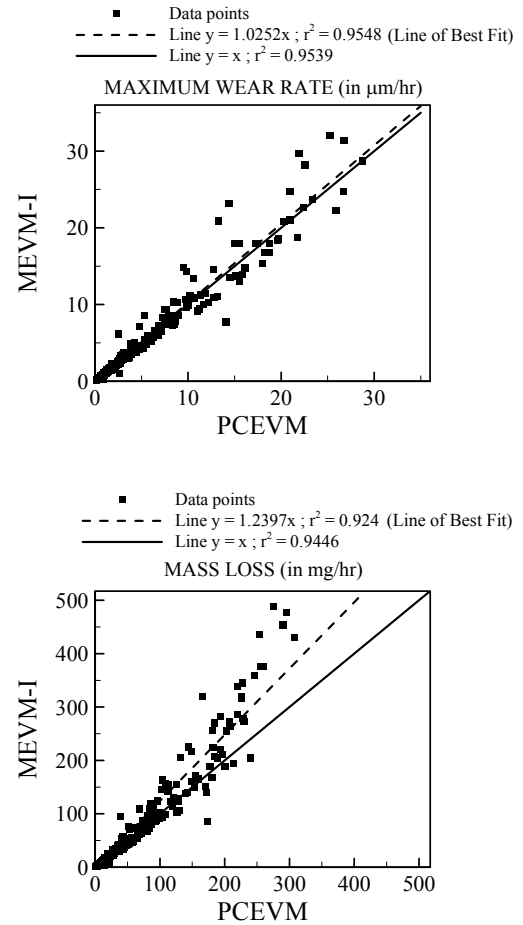


Fig. 2 Comparison of maximum wear rate (top) and mass loss (bottom) between PCEVM and MEVM-I

### B. Correlations

Based on the dataset obtained from parametric studies on wear, correlations are developed for the maximum wear rates for each model. These correlations are developed using the finite element (FE) generated data. The PSD is represented by the weighted mean diameter of the particles (Refer Table II). The FE generated data (using each model) for maximum wear rate is correlated in the general form as

$$\dot{W}_{\max}^{COR} = A \left( \frac{d_w}{H} \right)^{n1} (C_{avg})^{n2} (Re_H)^{n3} (Ro_H)^{n4}, \quad (14)$$

where  $A$ ,  $n1$ ,  $n2$ ,  $n3$ , and  $n4$ , are determined so as to yield a least square best fit for mean square error. In developing the correlations, non-dimensional forms of operating parameters (such as wear rate, weighted-mean diameter, average inlet concentration, bulk flow Reynolds number and so on) are used. The maximum wear rate is non dimensionalized with respect to  $\rho_s U_o^3 / E_{SP}^o$ , where  $U_o$  is the inlet velocity and

$E_{SP}^o$  is the value of  $E_{SP}$  for a particle of diameter  $270 \mu\text{m}$ , which is chosen as a reference particle. The root mean square error is calculated as follows

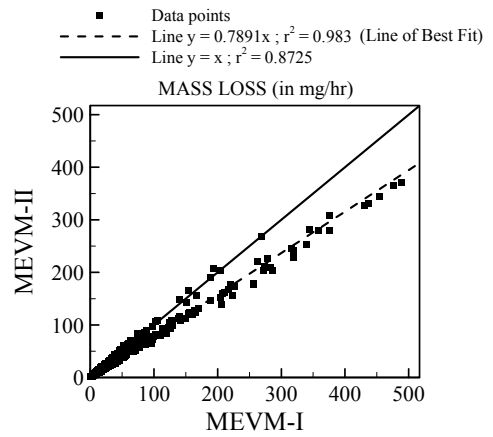
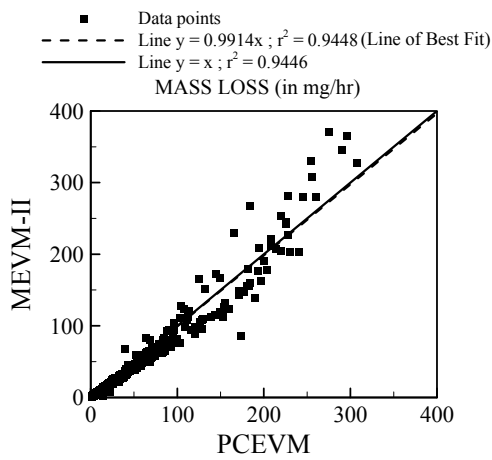
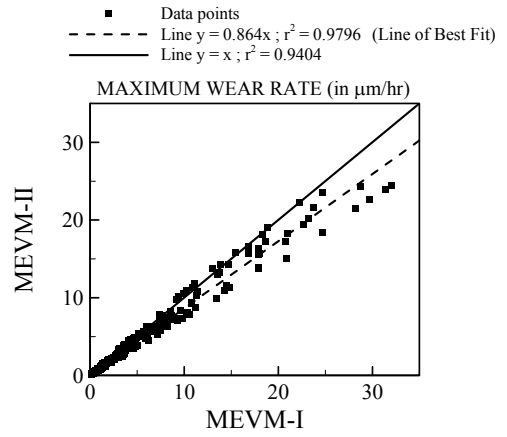
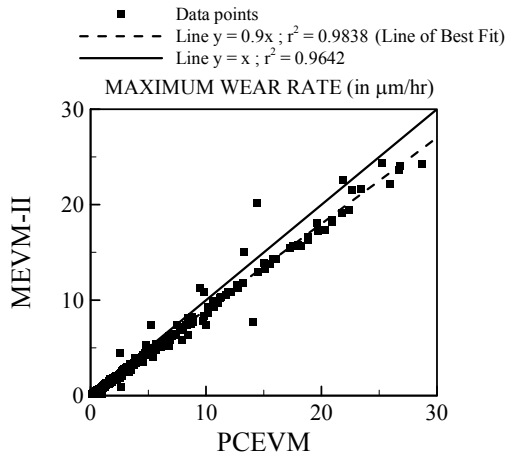


Fig. 4. Comparison of maximum wear rate (top) and mass loss (bottom) between MEVM-I and MEVM-II

Fig. 3. Comparison of maximum wear rate (top) and mass loss (bottom) between PCEVM and MEVM-II

$$\% \text{age RMS Error} = \sqrt{\frac{\sum_{i=1}^n \left( \frac{\dot{W}_{FE} - \dot{W}_{COR}}{\dot{W}_{FE}} \right)^2}{n}} \times 100, \quad (15)$$

where  $\dot{W}_{FE}$  is the finite element computed wear rate using each of the models,  $\dot{W}_{COR}$  is the corresponding value determined by correlation, and  $n$  is the number of data points. The correlation thus obtained using the least square linear regression for the three models PCEVM, MEVM-I and MEVM-II are, respectively,

### 1. PCEVM

$$\left[ \dot{W}_{\max}^{COR} \right]_{\text{PCEVM}} = 199.0018 \left( \frac{d_w}{H} \right)^{1.6764} (C_{avg})^{0.8818} (\text{Re}_H)^{-0.027} (\text{Ro}_H)^{0.2569}, \quad (16)$$

### 2. MEVM-I

$$\left[ \dot{W}_{\max}^{COR} \right]_{\text{MEVM-I}} = 199.924 \left( \frac{d_w}{H} \right)^{1.6781} (C_{avg})^{1.0076} (\text{Re}_H)^{-0.0108} (\text{Ro}_H)^{0.2396}, \quad (17)$$

and

### 3. MEVM-II

$$\left[ \dot{W}_{\max}^{COR} \right]_{\text{MEVM-II}} = 199.92 \left( \frac{d_w}{H} \right)^{1.7015} (C_{avg})^{0.8629} (\text{Re}_H)^{-0.0368} (\text{Ro}_H)^{0.2214}. \quad (18)$$

The RMS errors for the three correlations are 2.2%, 2.37% and 1.4% respectively. Fig. 5 shows the comparison of the FE generated data for maximum wear rate with the correlated data for all 432 cases using each of the three models, PCEVM, MEVM-I and MEVM-II. The regression coefficient ( $r^2$ ) for the line  $y = x$  is 0.9165 for PCEVM, 0.9222 for MEVM-I and 0.9222 for MEVM-II. The regression coefficients for both  $y = x$  (line of 100% accuracy) and the line of best fit indicate very good match

between the computed and correlated data for maximum wear rate. Needless to say, the correlations are likely to have reasonable accuracy only in the range of operating parameters over which finite element results have been generated.

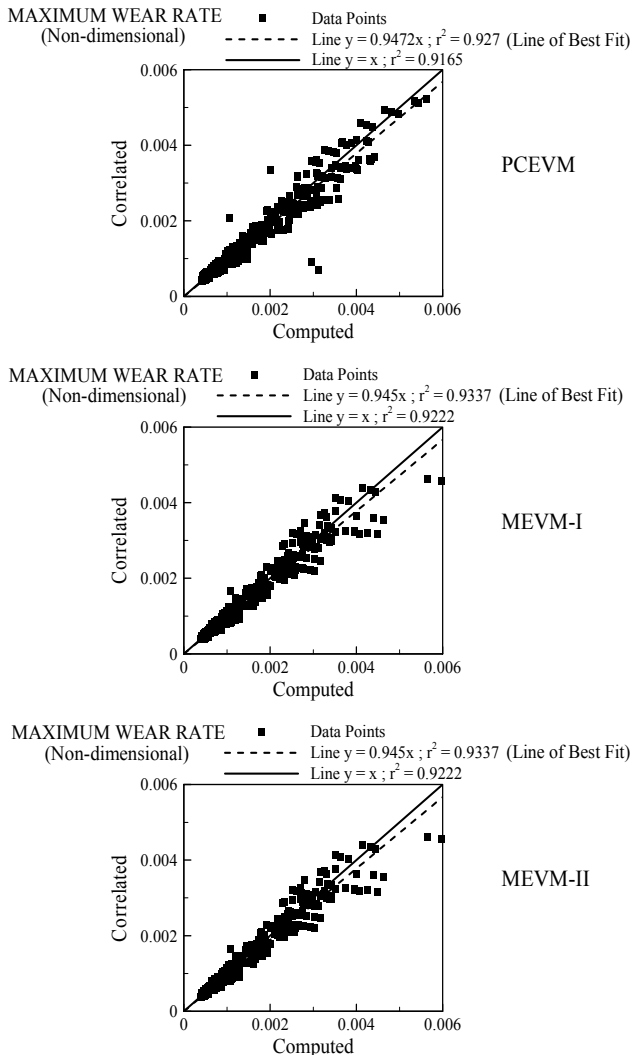


Fig. 5. Comparison of computed and correlated maximum wear using PCEVM (top), MEVM-I (center) and MEVM-II (bottom).

## V. CONCLUSIONS

Three variants of the two-equation  $k-\varepsilon$  model for turbulence have been used in erosion wear prediction of dense multi-size particulate flow through rotating channel. All the three turbulence modeling approach incorporates rotation modification to the production term in the turbulent kinetic energy equation.

Wear models have been modeled as a function of the local flow conditions and particle size-dependent wear coefficients (obtained from the open literature) for the chosen slurry/material combination (sand slurry and white iron alloy material).

A quantitative comparison of the wear rates predicted using

three turbulence models is made. It is shown that wear results using PCEVM and MEVM-I exhibit good agreement.

Finally correlations are developed between maximum wear rate and the operating parameters for all the three models. The RMS relative %age error between the FE-generated data and the correlations is found less than 2.5% for all the three models.

## ACKNOWLEDGMENT

The present work is a part of the original research carried out at the Department of Applied Mechanics, Indian Institute of Technology Delhi, New Delhi, India.

## REFERENCES

- [1] K. V. Pagalthivarthi and G. R. Addie, "Prediction methodology for two-phase flow and erosion wear in slurry impellers", *4th International Conference on Multiphase Flow, ICMF-2001*, New Orleans, LA, May 27-June 1, 2001.
- [2] G. R. Addie, A. Sellgren, J. Mudge, "SAG mill pumping cost considerations. SAG Conference", *3rd International Conference on Autogenous & Semiautogenous Grinding Technology*, September 30 – October 3, 2001, Vancouver, B.C., Canada, 2001.
- [3] G. R. Addie and A. Sellgren, "Effect of wear on the performance of centrifugal slurry pumps", *ASME Fluids Engineering Summer Meeting*, Washington, D.C., 1998.
- [4] D.R. Kaushal, V. Seshadri, S.N. Singh, "Prediction of concentration and particle size distribution in the flow of multi-sized particulate slurry through rectangular duct", *Appl. Math. Model.*, Vol. 26, No. 10, pp. 941-952, 2002.
- [5] J.S. Ravichandra, K.V. Pagalthivarthi, S. Sanghi, "Finite Element Study of Multi-size Particulate Flow in Horizontal Pipe", *Progress in Computational Fluid Dynamics*, Vol. 4, Issue 6, pp. 299-308, 2004.
- [6] J.S. Ravichandra, K.V. Pagalthivarthi, S. Sanghi, "Multi-size particulate flow in horizontal ducts – modeling and validation", *Progress in Computational Fluid Dynamics*, Vol. 5, Issue 8, pp. 466-481, 2005.
- [7] P.K. Gupta and K.V. Pagalthivarthi, "Finite Element Modelling and Simulation of Multi-Size Particulate Flow through Rotating Channel", *Progress in Computational Fluid Dynamics*, Vol. 7, Issue 5, pp. 247-260, 2007.
- [8] P.K. Gupta and K.V. Pagalthivarthi, "Application of Multifrontal and GMRES Solvers for Multi-Size Particulate Flow in Rotating Channels", *Progress in Computational Fluid Dynamics*, Vol. 7, Issue 5, pp. 323-336, 2007.
- [9] P.K. Gupta and K.V. Pagalthivarthi, "Effect of inlet concentration on solid-liquid mixture flow through rotating channel" In *Proceedings of International Congress on Computational Mechanics and Simulation – 2006*, December 8-10, 2006, IIT Guwahati, India, 2006.
- [10] P.K. Gupta and K.V. Pagalthivarthi, "Effect of particle size distribution on multi-size particulate flow through rotating channel" In *Proceedings of NCFMFP 33<sup>rd</sup> National and 3<sup>rd</sup> International Conference on Fluid Mechanics and Fluid Power*, December 7-9, 2006, IIT Bombay, India, 2006.
- [11] P.K. Gupta and K.V. Pagalthivarthi, "Effect of Diffusive Stress, Lift and Virtual Mass Forces on Multi-size Particulate Flow through Rotating Channel", in: Dwivedy, S. K. and Maity, D., ed(s), *Proceedings of International Congress on Computational Mechanics and Simulation*, December 8-10, 2006, IIT Guwahati, India, 2006.
- [12] M.C. Roco and C.A. Shook, "Modeling of Slurry Flow: The Effect of Particle Size" *Canadian Journal of Chemical Engineering*, Vol. 61, pp. 494-503, 1983.
- [13] M.C. Roco and C.A. Shook, "Computational Model for Coal Slurry Pipelines with Heterogeneous Size Distribution", *Powder Technology*, Vol. 39, pp. 159-176, 1984.
- [14] S.L. Soo, "Development of Theories on Liquid-Solid Flows," in: Roco, M.C., ed., *ASME-FED*, Vol. 13, 1984, pp. 1-6, 1984.
- [15] K.V. Pagalthivarthi, P.V. Desai, G.R. Addie, "Particulate Motion and Concentration Fields in Centrifugal Slurry Pumps", *Particulate Science and Technology*, Vol. 8, pp. 77-96, 1990.

- [16] M.C. Roco and E. Reinhardt, "Calculation of Solid Particle Concentration in Centrifugal Impellers using Finite Element Technique", in: *Proc. Hydrotransport 7 Conf.*, 1980, BHRA, pp. 359-376, 1980.
- [17] Y. Zhong Sen and Er. Lai Min, "Computation of Solid Particles Velocity and Concentration in Centrifugal Pump Impellers using Finite Element Method", *International Conference on Pumps and Systems*, Beijing, China, May 1992, paper number K4, pp. 513-526, 1992.
- [18] K.V. Pagalthivarthi and V.R. Ramanathan, "Finite Element Study of Two-phase Free Surface Flow in Rotating Channel", in: *Proc. Int. Conf. Multiphase Flows*, May 27-June 1, 2004, Tokyo, Japan, Paper No. 294, 2004.
- [19] K.V. Pagalthivarthi and P.K. Gupta, "Simulation of Developing Flow through Rotating Channel using  $Q_1, Q_0$  Finite Elements", *Progress in Computational Fluid Dynamics*, Vol. 4, Issue 6, pp. 285-298, 2004.
- [20] P.K. Gupta and K.V. Pagalthivarthi, "Comparison of Zero-equation and Two-equation  $k-\epsilon$  Model in Rotating Channel Flow", in: *Proc. 2<sup>nd</sup> BSME-ASME Int. Conf. Thermal Engg.*, 2-4 January, 2004, Dhaka, 2004.
- [21] J.H.G. Howard, S.V. Patankar, R.M. Bordyniuk, "Flow Prediction in Rotating Ducts using Coriolis-modified Turbulence Models", *ASME J. Fluids Engineering*, vol. 102, pp. 456-461, 1980.
- [22] K.V. Pagalthivarthi and P.K. Gupta, "Prediction of erosion wear in multi-size particulate flow through rotating channels" *Fluid Dynamics & Materials Processing*, vol. 5, issue 1, pp.93-122, 2009.
- [23] P.K. Gupta and K.V. Pagalthivarthi, "Multi-size particulate flow in rotating channels – Modelling and validation using three turbulence models" *Journal of Computational Multiphase Flows*, vol. 1, No. 2, pp. 133-160, 2009.
- [24] M. Manninen, V. Taivassalo, S. Kallio, "On the Mixture Model for Multiphase Flow", VTT Publications 288, Technical Research Centre of Finland, Espoo, pp. 1-67, 1996.
- [25] S. Kallio, M. Manninen, V. Taivassalo, "Turbulence in Mixture Models", Report :98-1, Åbo Akademi, Department of Chemical Engineering, Åbo, 1-31, 1998.
- [26] R. Visintainer, K.V. Pagalthivarthi, H.H. Tian, "Wear coefficient's dependence on particle size" GIW Internal Report, 2005.
- [27] H.H. Tian, G.R. Addie, K.V. Pagalthivarthi, "Determination of wear coefficients for prediction through Coriolis wear testing", *WEAR*, Vol. 259, pp. 160-170, 2005.
- [28] K.V. Pagalthivarthi and R. Veeraghavan, "Numerical insight into experimental results of particle size effect in Coriolis wear tester" *Proc. of the First International FMFP Conference, 15-17 Dec., 1998*, IIT Delhi, New Delhi, 1998.